

ChemComm

Accepted Manuscript



This is an *Accepted Manuscript*, which has been through the Royal Society of Chemistry peer review process and has been accepted for publication.

Accepted Manuscripts are published online shortly after acceptance, before technical editing, formatting and proof reading. Using this free service, authors can make their results available to the community, in citable form, before we publish the edited article. We will replace this *Accepted Manuscript* with the edited and formatted *Advance Article* as soon as it is available.

You can find more information about *Accepted Manuscripts* in the [Information for Authors](#).

Please note that technical editing may introduce minor changes to the text and/or graphics, which may alter content. The journal's standard [Terms & Conditions](#) and the [Ethical guidelines](#) still apply. In no event shall the Royal Society of Chemistry be held responsible for any errors or omissions in this *Accepted Manuscript* or any consequences arising from the use of any information it contains.

COMMUNICATION

Pyrene-based mechanically interlocked SWNTs.

Cite this: DOI: 10.1039/x0xx00000x

Alejandro López-Moreno and Emilio M. Pérez*

Received 00th January 2012,

Accepted 00th January 2012

DOI: 10.1039/x0xx00000x

www.rsc.org/

The synthesis of rotaxane-type species composed of pyrene macrocycles and SWNTs as linear components is described. Pyrene-SWNT interactions help template the ring-closing metathesis of U-shape precursors around the nanotubes.

Single wall carbon nanotubes (SWNTs) are rolled-up graphene sheets, forming tubules of diameter typically around 1 nm. SWNTs can be semiconducting or metallic depending on the direction of the honeycomb pattern along which the graphene sheet is rolled.¹ Metallic SWNTs show ballistic electron transport.² Semiconducting SWNTs have structurally inherent band-gaps, and their electrical properties are extremely sensitive to their surroundings, which have made them suitable as active materials in field effect transistors,³ photovoltaic devices,⁴ sensors,⁵ etc.⁶ Biomedical uses of carbon nanotubes,⁷ and nanotube-polymer composites⁸ are particularly active areas of research, too.

Considering all these potential fields of application, significant efforts have been devoted to the chemical modification of SWNTs in order to better exploit their extraordinary properties.⁹ A broad variety of strategies have been employed to attach molecular fragments to the surface of SWNTs via covalent¹⁰ and noncovalent methods.¹¹ Even the interior cavity of SWNTs has been functionalized.¹²

Rotaxanes are mechanically interlocked molecules (MIMs) composed of a linear constituent (thread) encapsulated by one or more macrocycles, which cannot escape without the breaking of a covalent bond. Since the macrocycle(s) can move along (shuttling) or around (pirouetting) the thread, rotaxanes have been investigated for the construction of synthetic molecular machines.¹³ Besides their dynamic properties, the mechanical link often results in distinct properties, which has spurred interest into mechanically interlocked materials. Ever since the pioneering work of Jean-Pierre Sauvage,¹⁴ the synthesis of MIMs typically relies on templated methods, in which supramolecular interactions preorganize the submolecular components towards the formation of the mechanical link.¹⁵

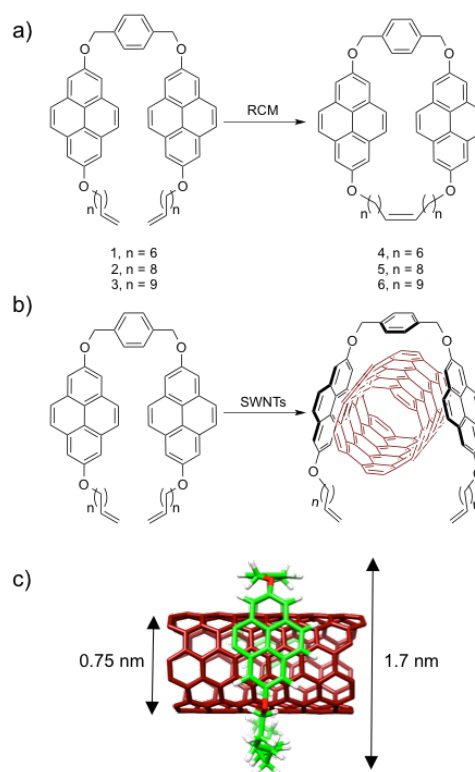


Fig. 1 a) Chemical structures of U-shapes 1-3 and macrocycles 4-6. b) Template effect in the macrocyclization of the U-shapes around SWNTs through pyrene-SWNT interactions. c) Energy-minimized (MM+) model of MINT-(6,5)-6 showing key distances.

We have recently reported the synthesis of rotaxane-type structures in which SWNTs act as threads, introducing the mechanical bond as a new tool for the chemical manipulation of SWNTs.¹⁶ To achieve this, we employed a clipping strategy in which a U-shape precursor

featuring two units of a recognition element for SWNTs were connected through an aromatic spacer, and further decorated with alkene-terminated alkyl spacers of different lengths. In particular, we used π -extended derivatives of tetrathiafulvalene (exTTF), which are known to establish positive noncovalent interactions with SWNTs,¹⁷ to template the ring closing metathesis (RCM) of the U-shape precursor around the SWNTs, forming mechanically interlocked derivatives of SWNTs (MINTs). The MINTs showed remarkable stability, comparable to that of covalently modified nanotubes, while maintaining the native structure of the SWNTs.

In order to investigate the scope of the MINT-forming reaction, we decided to test other molecular fragments known to interact with SWNTs. Here, we report that pyrene is a valid recognition motif for the synthesis of MINTs.

The U-shape precursors of the bispyrene macrocycles (**1-3**, Figure 1a) were synthesized by two consecutive Williamson's etherifications from 2,7-dihydroxy-pyrene¹⁸. Macrocycles **4-6** were synthesized by RCM and show flexible cavities of diameters ca. 1.4-1.8 nm as calculated from molecular mechanics (see ESI for synthetic details). We expected the SWNTs to template the macrocyclization of the U-shapes around them through pyrene-SWNT supramolecular interactions (Figure 1b). Accordingly, we tested (6,5) and (7,6)-enriched SWNTs as threads, which show diameters of 0.75 nm and 0.88 nm respectively and are a good fit for our macrocycles (Figure 1c). The SWNTs (5 mg) were suspended in tetrachloroethane (TCE, 5 mL) through sonication and mixed with the corresponding U-shapes **1-3** (2.5 mg) and Grubbs' second-generation catalyst at room temperature for 72 h. After this period, samples were filtered through a polytetrafluoroethylene membrane of 0.2 μm pore size. The solid was resuspended in CH_2Cl_2 with sonication, and washed profusely with CH_2Cl_2 to remove any unreacted linear precursors, non-interlocked macrocycles, weakly adsorbed pyrene materials, remaining catalyst, etc. This purification stage was repeated three times, after which the samples were dried and subjected to thermogravimetric analysis (TGA) to quantify the degree of functionalization. The results are summarized in Table 1 (see the ESI for all TGAs).

All samples show a significant weight loss (24-28 %) around 360 °C corresponding to pyrene material. This degree of functionalization is similar to that found for exTTF-based MINTs.¹⁶ Although the changes are quantitatively small, for a given type of SWNT the degree of functionalization increases consistently with the size of the macrocycle cavity, for instance MINT-(6,5)-**4** shows a 24% loading compared to 27% for MINT-(6,5)-**6**. The comparison between nanotube types shows that the (7,6)-SWNTs bear more macrocycle loading. Considering that both chiralities fit within the macrocycles, this tendency is most likely due to a more efficient U-shape-SWNT interaction, as it is known that the pyrene-SWNT interaction increases with increasing SWNT diameter.¹⁹ We also carried out control experiments in which we mixed linear precursor **3** or the corresponding macrocycle **6** with (7,6) SWNTs without Grubbs' catalyst, under otherwise identical conditions to the MINT-forming reaction. These samples showed a functionalization of 7 and 5 % respectively, proving that physisorbed **3** or **6** are only a minor part of the pyrene material in the MINT-**6** samples.

Table 1 Functionalization of the MINT and control samples from TGA.^a

U-shape	SWNT	MINT	Weight loss (%) ^b
1	(6,5)	MINT-(6,5)- 4	24 (21)
1	(7,6)	MINT-(7,6)- 4	25 (21)
2	(6,5)	MINT-(6,5)- 5	26 (22)
2	(7,6)	MINT-(7,6)- 5	27 (23)
3	(6,5)	MINT-(6,5)- 6	27 (25)
3	(7,6)	MINT-(7,6)- 6	28 (25)

^a TGAs were run in air at a heating rate of 10 °C/min. ^b All reactions were run twice, with reproducible results. Numbers in brackets were obtained after refluxing each sample in TCE, as described in the main text.

We have previously observed that MINTs show remarkable stability, comparable to that of covalently modified nanotubes, while maintaining the native covalent structure of the SWNTs.¹⁶ To test the stability of the functionalization and remove any remaining non-interlocked pyrene material that might have survived the initial purification process, we subjected all samples to 30 min of reflux in tetrachloroethane (TCE, bp = 147 °C), followed by a thorough rinse with CH_2Cl_2 . Such treatment should remove all non-interlocked pyrene materials. TGA of the resulting samples showed very small decrease in the degree of functionalization (< 4%, numbers in brackets in Table 1), confirming the extreme stability of MINTs, and that the supramolecular functionalization of the nanotubes by linear oligomers formed in situ under the RCM metathesis conditions is minority.¹⁶

Raman spectroscopy (λ_{exc} = 532, 633, and 785 nm) reveals very small changes to the spectra with respect to pristine SWNTs, as expected for the noncovalent functionalization of SWNTs with pyrene-based fragments.²⁰ In particular, we observed no significant increase in the $I_{\text{D}}/I_{\text{G}}$ ratio and no decrease in the RBM intensity, which confirm that there is no covalent modification of the SWNTs.²¹ We also observed a small shift of the G^+ band and a decrease in the relative intensity of the G^- band.^{19a} These changes are summarised in Table 2 and illustrated by Figure 2a, which shows the Raman spectra of the (7,6)-SWNT and MINT-(7,6)-**6** under 785 nm excitation. In this case, the $I_{\text{D}}/I_{\text{G}}$ ratio is 0.05 for the (7,6) SWNTs and 0.06 for MINT-(7,6)-**6**, while the G^+ band is shifted from 1578 to 1580 cm^{-1} (see the ESI for all Raman spectra).

In the absorption spectra (D_2O , 1% sodium dodecyl sulphate, 298 K, Figure 2b), the UV region is dominated by the nanotube absorption, and the characteristic absorption of pyrene in the 300-350 nm range is not distinguishable, save for an increase in the relative absorption in this region.[†] The S_{22} and S_{11} transitions of the (6,5)-SWNTs are prominent in the vis-NIR, appearing at λ_{max} = 572 and 991 nm for the pristine nanotubes. As expected for an intimate pyrene-SWNT supramolecular interaction both transitions are red shifted upon derivatization to form MINT-(6,5)-**6** to λ_{max} = 577 and 1006 nm, respectively, with the S_{22} suffering a quantitatively smaller shift due to its higher energy.²²

The photoluminescence excitation (PLE) maps of the (6,5)-enriched SWNTs show an intense peak at λ_{exc} = 565 nm, λ_{em} = 975 nm characteristic of the (6,5) chirality, and residual peaks at λ_{exc} = 643 nm, λ_{em} = 1021 nm and λ_{exc} = 665, λ_{em} = 948 nm, corresponding to (7,5) and (8, 3) chiralities. In MINT-(6,5)-**6**, the luminescence of the (6,5) nanotubes is quenched to approximately 40% and suffers a bathochromic shift to λ_{em} = 986 nm, compared to a sample of pristine (6,5) SWNTs with identical optical density (see the ESI).

The TGA data, control experiments, and spectroscopic characterization are therefore consistent with the formation of MINTs.¹⁶

Table 2 Selected Raman data for the MINT-6 samples.^a

Sample	532 nm		633 nm		785 nm	
	I _D /I _G	G ⁺	I _D /I _G	G ⁺	I _D /I _G	G ⁺
(6,5)	0.06	1572	0.08	1578	0.07	1577
MINT-(6,5)-6	0.07	1573	0.09	1579	0.08	1583
(7,6)	0.06	1568	0.07	1584	0.05	1578
MINT-(7,6)-6	0.08	1568	0.07	1586	0.06	1580

^a Average of at least three different Raman spectra. G⁺ Raman shifts in cm⁻¹.

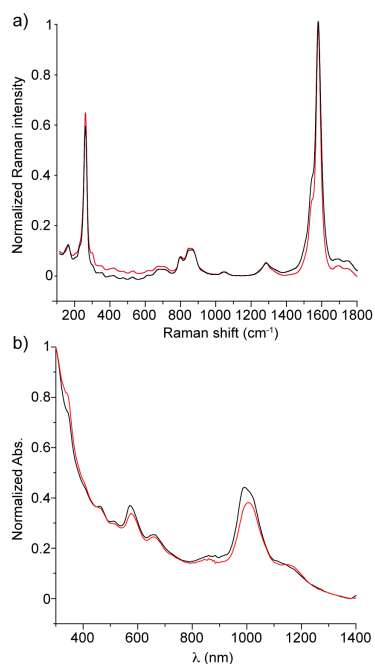


Fig. 2. a) Raman spectra ($\lambda_{\text{exc}} = 785 \text{ nm}$) of (7,6)-SWNTs (black) and MINT-(7,6)-6 (red). b) UV-vis-NIR (D_2O , 1% sodium dodecyl sulphate, 298 K) of (6,5)-SWNTs and MINT-(6,5)-6.

High-resolution transmission electron microscopy (HR-TEM) has proven to be a valuable tool to image organic molecules in the vicinity of carbon nanotubes,²³ and we have shown this is also the case for MINTs.¹⁶ Scrutiny under HR-TEM of samples of MINT-(6,5)-6 dropcasted from a TCE suspension shows mostly bundled nanotubes with heavily functionalized sidewalls, in agreement with the TGA data. A representative image is shown in Figure 3a, where two bundles and an isolated SWNT are distinguishable. Both the bundles and the single nanotube show abundant organic functionalization. For the free nanotube, a diameter of 0.8 nm was measured at its leftmost extreme, where it shows no addends; the derivatized part has a diameter of ca. 2 nm, in good agreement with multiple units of **6**, the first of which is sufficiently detached to be distinguishable. In several instances the nanotubes showed single circular objects of diameter $< 2 \text{ nm}$ around them. For example, Figure 3b shows a SWNT of diameter 0.7 nm in which up to four of these objects are visible. The size and shape of the addends is perfectly consistent with the formation of **6** around the SWNT (Figure 1c). Figures 3c and d further illustrate the formation of

rotaxane-type species. In Figure 3c a long SWNT of 0.7 nm in diameter shows two single objects of 1.8 and 1.7 nm, while in 3d we measured diameters of 0.8 and 1.9 nm for the nanotube and macrocycle, respectively. The role of the nanotube bundles as stoppers is also evident from the micrographs. Note that the discontinuity between the walls of the SWNT and the macrocycles is evident, particularly in Figures 3b and 3d. Together with their consistent size of 1.7-1.9 nm this rules out the possibility of them being SWNT imperfections.

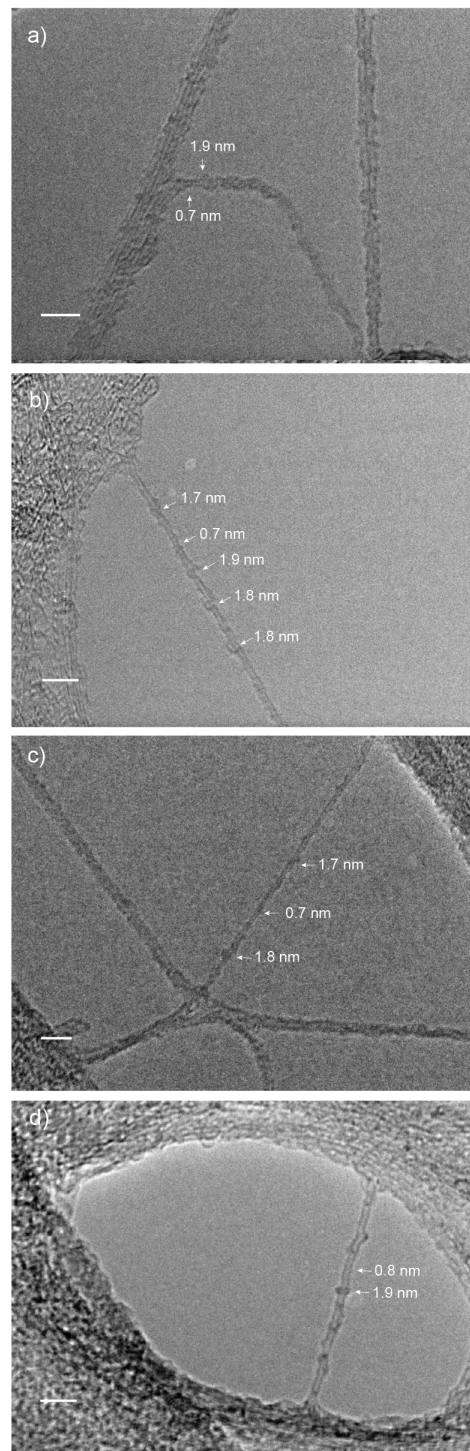


Fig. 3. Representative HR-TEM images of MINT-(6,5)-6. All scale bars are 5 nm.

In conclusion, we have proven that pyrene templates the RCM of macrocycles around SWNTs to form MINTs. The results disclosed here suggest that our clipping strategy towards the synthesis of MINTs might be applicable to any molecular fragment that shows sufficiently strong noncovalent interactions with SWNTs, and can be elaborated to synthesize appropriate U-shape precursors. This broad scope, together with the unique features of MIMs²⁴ and the interest in the encapsulation of carbon nanomaterials,²⁵ make the formation of MINTs a particularly attractive method for the noncovalent functionalization of SWNTs.

This work has been supported by the European Research Council (StG-2012, MINT-307609) and the Spanish MINECO (CTQ2011-25714).

Notes and references

IMDEA Nanociencia, C/Faraday 9, Ciudad Universitaria de Cantoblanco, 28049, Madrid, SPAIN. E-mail: emilio.perez@imdea.org.

† The extinction coefficient for pyrene in aqueous environment is varies between 21000 and 34000 M⁻¹ cm⁻¹,²⁶ while it is 4400 M⁻¹ cm⁻¹ per carbon atom for the S₁₁ transition of (6,5) SWNTs,²⁷ which shows half the absorption of the 300-400 nm region. At 26% functionalization, we estimate approximately one unit of **6** every 200 SWNT carbon atoms, so the absorption of the SWNT should be ca. 10 times larger than pyrene.

Electronic Supplementary Information (ESI) available: Experimental details, characterization, and supporting figures. See DOI: 10.1039/c000000x/

- H. Dai, *Acc. Chem. Res.*, 2002, **35**, 1035-1044.
- J. Kong, E. Yenilmez, T. W. Tombler, W. Kim, H. Dai, R. B. Laughlin, L. Liu, C. S. Jayanthi and S. Y. Wu, *Phys. Rev. Lett.*, 2001, **87**, 106801.
- A. Wurl, S. Goossen, D. Canevet, M. Sallé, E. M. Pérez, N. Martín and C. Klinke, *J. Phys. Chem. C*, 2012, **116**, 20062-20066.
- (a) M. Bernardi, J. Lohrman, P. V. Kumar, A. Kirkeminde, N. Ferralis, J. C. Grossman and S. Ren, *ACS Nano*, 2012, **6**, 8896-8903; (b) H. Wang, G. I. Koleilat, P. Liu, G. Jiménez-Oses, Y.-C. Lai, M. Vosgueritchian, Y. Fang, S. Park, K. N. Houk and Z. Bao, *ACS Nano*, 2014, **8**, 2609-2617.
- (a) B. Esser, J. M. Schnorr and T. M. Swager, *Angew. Chem., Int. Ed.*, 2012, **51**, 5752-5756; (b) A. M. Münzer, Z. P. Michael and A. Star, *ACS Nano*, 2013, **7**, 7448-7453.
- For recent reviews, see: (a) J. M. Schnorr and T. M. Swager, *Chem. Mater.*, 2011, **23**, 646-657; (b) S. Park, M. Vosguerichian and Z. Bao, *Nanoscale*, 2013, **5**, 1727-1752; (c) C. Wang, K. Takei, T. Takahashi and A. Javey, *Chem. Soc. Rev.*, 2013, **42**, 2592-2609.
- (a) G. Cellot, E. Cilia, S. Cipollone, V. Rancic, A. Sucapane, S. Giordani, L. Gambazzi, H. Markram, M. Grandolfo, D. Scaini, F. Gelain, L. Casalis, M. Prato, M. Giugliano and L. Ballerini, *Nat. Nanotechnol.*, 2009, **4**, 126-133; (b) M. Adeli, R. Soleyman, Z. Beiranvand and F. Madani, *Chem. Soc. Rev.*, 2013, **42**, 5231-5256.
- (a) J. N. Coleman, U. Khan, W. J. Blau and Y. K. Gun'ko, *Carbon*, 2006, **44**, 1624-1652; (b) Z. Spitalsky, D. Tasis, K. Papagelis and C. Galiotis, *Prog. Polym. Sci.*, 2010, **35**, 357-401.
- (a) D. Tasis, N. Tagmatarchis, A. Bianco and M. Prato, *Chem. Rev.*, 2006, **106**, 1105-1136; (b) A. Hirsch, *Angew. Chem., Int. Ed.*, 2002, **41**, 1853-1859; (c) S. Niyogi, M. A. Hamon, H. Hu, B. Zhao, P. Bhowmik, R. Sen, M. E. Itkis and R. C. Haddon, *Acc. Chem. Res.*, 2002, **35**, 1105-1113.
- (a) C. A. Dyke and J. M. Tour, *J. Phys. Chem. A*, 2004, **108**, 11151-11159; (b) P. Singh, S. Campidelli, S. Giordani, D. Bonifazi, A. Bianco and M. Prato, *Chem. Soc. Rev.*, 2009, **38**, 2214-2230.
- (a) Y.-L. Zhao and J. F. Stoddart, *Acc. Chem. Res.*, 2009, **42**, 1161-1171; (b) G. Gavrel, B. Joussemle, A. Filoramo and S. Campidelli, *Top. Curr. Chem.*, 2014, **348**, 95-126.
- (a) A. de Juan and E. M. Pérez, *Nanoscale*, 2013, **5**, 7141-7148; (b) T. Zoberbier, T. W. Chamberlain, J. Biskupek, N. Kuganathan, S. Eyhusen, E. Bichoutskaia, U. Kaiser and A. N. Khlobystov, *J. Am. Chem. Soc.*, 2012, **134**, 3073-3079.
- (a) E. R. Kay, D. A. Leigh and F. Zerbetto, *Angew. Chem., Int. Ed.*, 2007, **46**, 72-191; (b) D. A. Leigh and E. M. Pérez, *Top. Curr. Chem.*, 2006, **265**, 185-208.
- (a) C. O. Dietrich-Buchecker, J. P. Sauvage and J. P. Kintzinger, *Tetrahedron Lett.*, 1983, **24**, 5095-5098; (b) C. O. Dietrich-Buchecker, J. P. Sauvage and J. M. Kern, *J. Am. Chem. Soc.*, 1984, **106**, 3043-3045.
- For reviews, see: (a) J. F. Stoddart, *Chem. Soc. Rev.*, 2009, **38**, 1802-1820; (b) M. S. Vickers and P. D. Beer, *Chem. Soc. Rev.*, 2007, **36**, 211-225; (c) C. O. Dietrich-Buchecker and J. P. Sauvage, *Chem. Rev.*, 1987, **87**, 795-810; For a recent selected example, see: (d) D. A. Leigh, R. G. Pritchard and A. J. Stephens, *Nat Chem*, 2014, **6**, 978-982.
- A. de Juan, Y. Pouillon, L. Ruiz-González, A. Torres-Pardo, S. Casado, N. Martín, A. Rubio and E. M. Pérez, *Angew. Chem., Int. Ed.*, 2014, **53**, 5394-5400.
- C. Romero-Nieto, R. García, M. Á. Herranz, C. Ehli, M. Ruppert, A. Hirsch, D. M. Guldi and N. Martín, *J. Am. Chem. Soc.*, 2012, **134**, 9183-9192.
- A. G. Crawford, Z. Liu, I. A. I. Mkhaliid, M.-H. Thibault, N. Schwarz, G. Alcaraz, A. Steffen, J. C. Collings, A. S. Batsanov, J. A. K. Howard and T. B. Marder, *Chem. Eur. J.*, 2012, **18**, 5022-5035, S5022/5021-S5022/5027.
- (a) S. G. Stepanian, V. A. Karachevtsev, A. Y. Glamazda, U. Dettlaff-Weglikowska and L. Adamowicz, *Mol. Phys.*, 2003, **101**, 2609-2614; (b) G. Modugno, Z. Syrgiannis, A. Bonasera, M. Carraro, G. Giancane, L. Valli, M. Bonchio and M. Prato, *Chem. Commun.*, 2014, **50**, 4881-4883.
- Y. Tomonari, H. Murakami and N. Nakashima, *Chem. Eur. J.*, 2006, **12**, 4027-4034.
- C. Fantini, M. L. Usrey and M. S. Strano, *J. Phys. Chem. C*, 2007, **111**, 17941-17946.
- M. S. Strano, C. B. Huffman, V. C. Moore, M. J. O'Connell, E. H. Haroz, J. Hubbard, M. Miller, K. Rialon, C. Kittrell, S. Ramesh, R. H. Hauge and R. E. Smalley, *J. Phys. Chem. B*, 2003, **107**, 6979-6985.
- E. Nakamura, *Angew. Chem., Int. Ed.*, 2013, **52**, 236-252.
- (a) E. A. Neal and S. M. Goldup, *Chem. Commun.*, 2014, **50**, 5128-5142; (b) J. F. Stoddart, *Angew. Chem., Int. Ed.*, 2014, **53**, 11102-11104.
- (a) S. Sato, T. Yamasaki and H. Isobe, *Proc. Natl. Acad. Sci. U. S. A.*, 2014, **111**, 8374-8379; (b) D. Canevet, E. M. Pérez and N. Martín, *Angew. Chem., Int. Ed. Engl.*, 2011, **50**, 9248-9259; (c) H. Isobe, S. Hitosugi, T. Yamasaki and R. Iizuka, *Chem. Sci.*, 2013; (d) D. Canevet, M. Gallego, H. Isla, A. de Juan, E. M. Pérez and N. Martín, *J. Am. Chem. Soc.*, 2011, **133**, 3184-3190.
- H. Siu and J. Duhamel, *J. Phys. Chem. B*, 2008, **112**, 15301-15312.
- F. Schöppler, C. Mann, T. C. Hain, F. M. Neubauer, G. Privitera, F. Bonaccorso, D. Chu, A. C. Ferrari and T. Hertel, *J. Phys. Chem. C*, 2011, **115**, 14682-14686.